2009

Mice lacking mannose 6-phosphate uncovering enzyme activity have a milder phenotype than mice deficient for N-acetylglucosamine-1-phosphotransferase activity

Marielle Boonen
Washington University School of Medicine in St. Louis

Peter Vogel
Lexicon Pharmaceuticals, Inc.

Kenneth A. Platt
Lexicon Pharmaceuticals, Inc.

Nancy Dahms
Medical College of Wisconsin

Stuart Kornfeld
Washington University School of Medicine in St. Louis

Molecular Biology of the Cell
Vol. 20, 4381–4389, October 15, 2009

Mice Lacking Mannose 6-Phosphate Uncovering Enzyme Activity Have a Milder Phenotype than Mice Deficient for *N*-Acetylglucosamine-1-Phosphotransferase Activity

Marielle Boonen,* Peter Vogel,† Kenneth A. Platt,† Nancy Dahms,‡ and Stuart Kornfeld*

*Department of Internal Medicine, Washington University School of Medicine, St. Louis, MO 63110; †Department of Pathology, Lexicon Pharmaceuticals, Inc., The Woodlands, TX 77381; and ‡Department of Biochemistry, Medical College of Wisconsin, Milwaukee, WI 53226

Submitted May 14, 2009; Revised July 28, 2009; Accepted August 17, 2009
Monitoring Editor: Sean Munro

The mannose 6-phosphate (Man-6-P) lysosomal targeting signal on acid hydrolases is synthesized by the sequential action of uridine 5′-diphosphate-*N*-acetylglucosamine: lysosomal enzyme *N*-acetylglucosamine-1-phosphotransferase (GlcNAc-1-phosphotransferase) and GlcNAc-1-phosphodiester α-*N*-acetylglucosaminidase ("uncovering enzyme" or UCE). Mutations in the two genes that encode GlcNAc-1-phosphotransferase give rise to lysosomal storage diseases (mucolipidosis type II and III), whereas no pathological conditions have been associated with the loss of UCE activity. To analyze the consequences of UCE deficiency, the UCE gene was inactivated via insertional mutagenesis in mice. The UCE −/− mice were viable, grew normally and lacked detectable histologic abnormalities. However, the plasma levels of six acid hydrolases were elevated 1.6- to 5.4-fold over wild-type levels. These values underestimate the degree of hydrolase hypersecretion as these enzymes were rapidly cleared from the plasma by the mannose receptor. The secreted hydrolases contained GlcNAc-P-Man diesters, exhibited a decreased affinity for the cation-independent mannose 6-phosphate receptor and failed to bind to the cation-dependent mannose 6-phosphate receptor. These data demonstrate that UCE accounts for all the uncovering activity in the Golgi. We propose that in the absence of UCE, the weak binding of the acid hydrolases to the cation-independent mannose 6-phosphate receptor allows sufficient sorting to lysosomes to prevent the tissue abnormalities seen with GlcNAc-1-phosphotranferase deficiency.

INTRODUCTION

In higher eukaryotes, mannose 6-phosphate (Man-6-P) monoesters on newly synthesized acid hydrolases serve as high-affinity ligands for binding to Man-6-P receptors (MPRs) in the *trans*-Golgi network (TGN). This is followed by packaging of the receptor–ligand complexes into transport carriers that deliver the acid hydrolases to endosomes where they are released and subsequently incorporated into lysosomes (for reviews, see Ghosh *et al*., 2003; Braulke and Bonifacino, 2009). The generation of the Man-6-P recognition signal is a two step process. First, uridine 5′-diphosphate-*N*-acetylglucosamine (UDP-GlcNAc):lysosomal enzyme *N*-acetylglucosamine-1-phosphotransferase (GlcNAc-1-phosphotransferase) transfers GlcNAc-P to selected mannose residues of the *N*-linked high mannose glycans on the acid hydrolases. Then, *N*-acetylglucosamine-1-phosphodiester α-*N*-acetylglucosaminidase ("uncovering enzyme" or UCE or "Nagpa") excises the GlcNAc to form the Man-6-P monoester. UCE is a type 1 transmembrane glycoprotein of 515 amino acids that localizes to the TGN but cycles to the plasma membrane (Varki and Kornfeld, 1981; Kornfeld *et al*., 1999; Rohrer and Kornfeld, 2001, Lee *et al*., 2002b). It is synthesized as an inactive precursor that is activated upon proteolytic cleavage by the TGN-localized endoprotease furin (Do *et al*., 2002).

Mutations in the two genes that encode the subunits (α/β and γ) of GlcNAc-1-phosphotransferase give rise to autosomal recessive lysosomal storage disorders (I-cell disease/mucolipidosis [ML]-II and PseudoHurler polydystrophy/ML-III) characterized by hypersecretion of lysosomal hydrolases, skeletal abnormalities, and psychomotor retardation (for review, see Kornfeld and Sly, 2000; Cathey *et al*., 2009). To date, there have been no reports of pathological mutations in the gene that encodes UCE. There are several potential explanations for this. There could be an alternative mechanism for conversion of the Man-6-P diesters to monoesters. Furthermore, inactivating mutations in the UCE gene might be very rare events. Finally, it was recently reported that repeat domain 5 (of a total of 15 repeating domains) of the cation-independent mannose 6-phosphate receptor (CI-MPR) is able to bind GlcNAc-P-Man diesters, although this binding was of much lower affinity than the binding of Man-6-P monoesters to domains 1–3 and 9 of the receptor (Chavez *et al*., 2007; for review, see Dahms *et al*., 2008). This raises the

This article was published online ahead of print in *MBC in Press* (http://www.molbiolcell.org/cgi/doi/10.1091/mbc.E09–05–0398) on August 26, 2009.

Address correspondence to: Stuart Kornfeld (skornfel@im.wustl.edu).

Abbreviations used: CD-MPR, cation-dependent mannose 6-phosphate receptor; CI-MPR, cation-independent mannose 6-phosphate receptor; GlcNAc, *N*-acetylglucosamine; GlcNAc-1-phosphotransferase, UDP-GlcNAc:lysosomal enzyme, *N*-acetylglucosaminyl-1-phosphotransferase; GNPTAB, GlcNAc-1-phosphotransferase α/βsubunits; HSA-mannose, human serum albumin-mannose; Man, mannose; ML, mucolipidosis; *Nagpa*, GlcNAc-1-phosphodiester alpha-N-acetylglucosaminidase; P, phosphate; TGN, *trans*-Golgi network; UCE, uncovering enzyme.

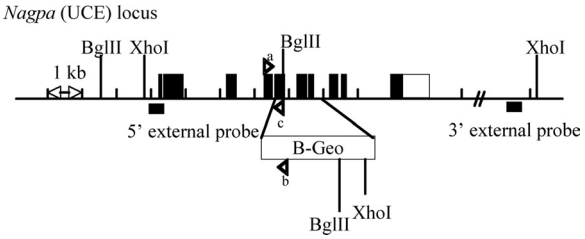

Figure 1. Disruption of the UCE gene by insertional mutagenesis. A β-galactosidase-Neomycin cassette (B-Geo) was inserted between exons 4 and 8 of the gene encoding UCE (*Nagpa*) in mouse, by using a targeting mutagenesis approach. The localization of the probes (5′- and 3′-external) and restriction sites (XhoI-BglII) used for the Southern blot experiment (see Figure 2A), and the primers used for genotyping the mice (see Figure 2B) are shown.

possibility that, in the absence of UCE activity, acid hydrolases bearing Man-6-P diesters might be able to bind sufficiently to the CI-MPR to allow enough trafficking to lysosomes to prevent the clinical manifestations seen with GlcNAc-1-phosphotransferase deficiency. However, these studies were performed in vitro; thus, it is not clear whether this low-affinity binding to the receptor would prevent hypersecretion of acid hydrolases by cells lacking UCE activity.

Mice with a disruption of the gene encoding the α/β subunits of GlcNAc-1-phosphotransferase have very high serum levels of acid hydrolases that lack Man-6-P monoesters (Gelfman *et al*., 2007; Lee *et al*., 2007). These mice exhibit growth retardation, severe retinal degeneration, and striking vacuolization of the secretory cells of several exocrine glands (Gelfman *et al*., 2007; Vogel *et al*., 2009). To analyze the consequences of the loss of UCE activity, we used insertional mutagenesis to inactivate the single gene encoding UCE in mice. Our results indicate that UCE accounts for essentially all the conversion of GlcNAc-P-Man diester to monoester on newly synthesized acid hydrolases. Loss of UCE activity induces hypersecretion of acid hydrolases but, in contrast to the loss of GlcNAc-1-phosphotransferase, there are no detectable growth or tissue abnormalities in these mice.

MATERIALS AND METHODS

Materials

Chemicals were obtained from Sigma-Aldrich (St. Louis, MO) unless otherwise specified. Recombinant human UCE, recombinant human GlcNAc-1-phosphotransferase along with human serum albumin-mannose were generously provided by Dr. W. Canfield (Genzyme, Oklahoma City, OK). The CI-MPR affinity column (CI-MPR coupled at 0.5 mg/ml Affigel-10 matrix) was prepared as described previously (Varki and Kornfeld, 1983). Cation-dependent (CD)-MPR (soluble, glycosylation-deficient form) was expressed in *Pichia pastoris* as a secreted protein, purified by pentamannosyl phosphate agarose affinity chromatography and coupled at 0.7 mg/ml to Affigel-10 matrix, as described previously (Reddy *et al*., 2003). Cellgro α-minimal essential media (α-MEM) and penicillin/streptomycin were obtained from Thermo Fisher Scientific (Waltham, MA). G418 sulfate was obtained from Calbiochem (EM Scientific, Gibbstown, NJ), and fetal calf serum (FCS) was from ISC BioExpress (Kaysville, UT).

Generation of Mutant Nagpa (UCE) Mice

The gene that encodes UCE in mice (*Nagpa*) was disrupted by insertional mutagenesis (Figure 1). The targeting vector was generated by insertion of two Nagpa-homology domains (5′ and 3′ arms) upstream and downstream of a β-galactosidase-Neomycin (B-Geo) cassette, respectively. The homology arms were derived using long-range polymerase chain reaction (PCR) using 129/SvEv^{Brd} embryonic stem (ES) cell (Lex-1) DNA as a template. The 3639 base pairs 5′ arm was generated using primers Nagpa-2 [5′-TAGCGGCCGCGACGCGATGGAACCATAGTCAC-3′] and Nagpa-1 [5′-ATGGCGCGCCATCTCCCATAGGTTAAGGCTGTGC-3′] and cloned using the TOPO (Invitrogen, Carlsbad, CA) cloning kit. The 4564-base pair 3′ arm was generated using primers Nagpa-6 [5′-ATGGCGCGCCGCAGCTGGTATGACGCCTTC-3′] and Nagpa-7 [5′-CTAAGCTTCAGAAAGGGCGCTCTCAGAGTAAC-3′] and cloned using the TOPO cloning kit. The 5′ arm was excised from the holding plasmid by using NotI and AscI. The 3′ arm was excised from the holding plasmid by using AscI and HindIII. The arms were ligated via AscI to a cassette containing a β-galactosidase-Neomycin fusion marker (B-Geo) along with a PGK promoter-driven puromycin resistance marker. The construct (5′-arm-B-Geo-3′-arm) was then inserted into a NotI/HindIII cut pKO Scrambler vector (Stratagene, La Jolla, CA) to complete the Nagpa targeting vector, which display a deletion of coding exons 5–7 (Figure 1). The NotI-linearized targeting vector was electroporated into 129/SvEv^{Brd} (Lex-1) ES cells. G418/FIAU-resistant ES cell clones were isolated, and their DNA was analyzed by Southern blot (see *Results*) by using a 289-base pair 5′ external probe (8/9) (Figure 1), generated by PCR using primers Nagpa-8 [5′-TGGAATTCGAATGCGTAATCAA-3′] and Nagpa-9 [5′-GTCATCGTCGCGGGAAA-3′], and a 236-base pair 3′ external probe (10/11) (Figure 1), amplified by PCR using primers Nagpa-10 [5′-ACTCAGGCAATGACTCGCTGTG-3′] and Nagpa-11 [5′-CCCGCTCCTCTCATAGACGCTA-3′]. Two targeted ES cell clones (1B10 and 1G7) were identified and microinjected into C57BL/6 (albino) blastocysts to generate chimeric animals that were bred to C57BL/6 (albino) females, and the resulting heterozygous offspring were interbred to produce homozygous *Nagpa*-deficient mice.

Comprehensive Phenotypic Screen

Wild-type and homozygous null mice were subjected to a comprehensive battery of phenotype screening exams as described previously (BeltrandelRio *et al*., 2003; Zambrowicz *et al*., 2003). Screening assays included behavioral tests (such as circadian rhythm, open field, inverted screen, prepulse inhibition of the acoustic startle response, tail suspension, marble burying, and context trace conditioning), funduscopy and retinal angiography exams, blood pressure and heart rate measurements, serum chemistries, insulin levels, glucose tolerance testing, hematology, peripheral blood fluorescence-activated cell sorting analysis, urinalysis, quantitative magnetic resonance, dual-energy x-ray absorptiometry scans, computerized axial tomography scans, microcomputed tomography scans, fertility testing, skin fibroblast proliferation assays, and pathology.

Histopathology

Immediately after euthanasia, knockout mice and age-matched normal control mice were fixed by cardiac perfusion with 10% neutral buffered Formalin. Tissues were collected and immersed in 10% neutral buffered Formalin for an additional 48 h except for the eyes, which were removed and fixed by immersion in Davidson's fixative (Poly-Scientific Research, Bay Shore, NY) overnight at room temperature. All tissues were embedded in paraffin, sectioned at 4 μm, and mounted on positively charged glass slides (Superfrost Plus; Thermo Fisher Scientific). Sections were stained with hematoxylin and eosin for histopathologic examination.

Enzyme Assays

Lysosomal hydrolase activities were determined by fluorometric enzyme assays as described previously (Gelfman *et al*., 2007). In brief, plasma samples were incubated with 5 mM 4-methylumbelliferyl-coupled specific substrates (or 1 mM for tissue samples) in a 50 mM citrate buffer containing 0.5% Triton X-100, pH 4.5, at 37°C. Reactions were stopped by addition of 0.1 M glycine-NaOH solution, pH 10.3, and the fluorescence read at 495 nm. For plasma levels, activities were expressed as nanomoles of hydrolyzed methylumbelliferone per hour per milliliter of plasma.

Percoll Density Gradients

Wild-type and UCE −/− mice that were 2–3 mo of age were anesthetized and then perfused with phosphate-buffered saline (PBS) to remove blood from their organs. The brains and livers of these mice were removed and homogenized in 0.25 M sucrose by using a Potter-Elvehjem homogenizer and centrifuged at 1000 × *g* for 10 min at 4°C. The pellet was resuspended in 2 ml of sucrose solution and centrifuged at 1000 × *g* for 10 min. The supernatants of these two steps were pooled (postnuclear fraction) and centrifuged at 35,000 rpm in a 50Ti rotor (Beckman Coulter, Fullerton, CA) for 40 min at 4°C. The resulting pellet (membrane fraction) was resuspended in 1 ml of sucrose solution. Then, 500 μl of this fraction was loaded on top of an 18% Percoll solution (18%, vol/vol Percoll [Pharmacia, Uppsala, Sweden], 0.25 M sucrose, 2 mM EDTA and 10 mM Tris-HCl, pH 7.4) and centrifuged at 25,000 rpm in an SW55Ti rotor (Beckman Coulter) for 40 min at 4°C. Seven fractions were collected from the top of the gradient. The distribution of four different lysosomal hydrolases was determined by enzyme assays as described above.

Plasma Lysosomal Hydrolases Clearance Assay

Plasma samples were collected before and 4 h after injection of 200 mg/kg human serum albumin-mannose into the tail vein of ~3-mo-old wild-type (WT), UCE −/− or GlcNAc-1-phosphotransferase (GNPTAB) −/− mice. Plasma lysosomal hydrolases activities were then determined as described above.

Cathepsin D Sorting Assay

Mouse skin fibroblasts were isolated from wild-type and UCE −/− mouse ears and maintained in α-MEM medium containing 20% FCS, 100 μg/ml penicillin, and 100 U/ml streptomycin. Confluent cells (36-mm wells) were incubated with 1 ml of methionine/cysteine-free α-MEM medium containing ~600 μCi of TRAN ^{35}S-LABEL methionine/cysteine (MP Biomedicals, Ivrine, CA) and 10% dialyzed FCS for 1.5 h. Then, a 4-h chase period was initiated by replacing the labeling medium with 1 ml of α-MEM containing 10% FCS and either 5 mM Man-6-P or 5 mM Man-6-P and 660 μg/ml human serum albumin (HSA)-mannose (~10 μM) to prevent internalization of secreted cathepsin D. Chase media were collected and cells were lysed in immunoprecipitation (IP) buffer (0.1 M Tris HCl, pH 8, 0.15 M NaCl, and 1% triton [TX]-100) containing proteases inhibitors. After centrifugation for 10 min at 14,000 rpm to remove the cell debris, the cell lysates and media were incubated overnight with 60 μl of protein A-Sepharose beads that had been preincubated with 2 μl of polyclonal rabbit anti-cathepsin D antibody for 4 h at 4°C. The next day, the beads were washed once with cold IP buffer and then three times with buffer containing 0.1 M Tris-HCl, pH 8.0, 1 M NaCl, 1% TX-100, and 2 mM EDTA, followed by one more time with IP buffer. Immunoprecipitated cathepsin D was released from the beads by boiling 5 min at 100°C in Laemmli's sample buffer without reducing agent. Samples were resolved on 10% SDS-polyacrylamide gel electrophoresis (PAGE), which was fixed in 30% methanol:10% acetic acid for 20 min and incubated with an amplification solution (Amplify; GE Healthcare, Little Chalfont, Buckinghamshire, United Kingdom) for 10 min before drying and exposure on a photographic film (ISC BioExpress). Bands were then excised from gel and incubated in formic acid:H_2O_2 (20%:32%, vol/vol) for 2 d at 55°C. Radioactivity was measured with a counter (Beckman Coulter LS 6000IC, Fullerton, CA).

Synthesis of N-Acetylglucosaminyl 6-phosphomethylmannose

α-Methylmannoside (100 mM) was incubated for 48 h at 37°C with 500 ng of purified GlcNAc-1-phosphotransferase, 19 mM unlabeled UDP-GlcNAc, and 25,000 counts of [^{3}H]UDP-GlcNAc in a final volume of 500 μl. Assay buffer was composed of 0.1 M Tris, pH 7.5, 0.1 M $MgCl_2$, 0.1 M $MnCl_2$, and 2 mg/ml bovine serum albumin (BSA). The reaction was stopped by boiling 5 min at 100°C. The sample was centrifuged for 10 min at 10,000 × *g*, and the supernatant was loaded onto a 25-ml QAE-Sephadex column (2.5 × 5.0 cm) equilibrated with 2 mM Tris-HCl, pH 8.0. The column was washed with 50 ml of equilibration buffer and then eluted with 140 ml of 30 mM NaCl and 2 mM Tris-HCl, pH 8.0, followed by 30 ml of 2 M NaCl and 2 mM Tris-HCl, pH 8.0. Fractions (3.5 ml) collected with the first elution buffer that contained tritium were pooled and lyophilized, and the GlcNAc-P-α-methylmannose product was solubilized with water and passed over a P-2 column to remove salt (Bio-Rad Laboratories, Hercules, CA).

CD- and CI-MPR Affinity Chromatography

Plasma samples (50–100 μl) were diluted 10-fold in CI-MPR column buffer (50 mM imidazole, pH 6.5, 0.15 mM NaCl, and 0.05% TX-100) or CD-MPR column buffer (same as CI-MPR buffer + 5 mM β-glycerophosphate and 10 mM $MnCl_2$) and loaded on a CI-MPR affinity column (0.5 mg CI-MPR/ml Affigel-10) or CD-MPR affinity column (0.7 mg CD-MPR/ml Affigel-10) prepared as described previously (Varki and Kornfeld, 1983; Reddy *et al.*, 2003). Columns were washed with 7 ml of column buffer and then with 7 ml of column buffer containing 5 mM Glc-6-P, and finally with 5 ml of column buffer containing 10 mM Man-6-P. One-milliliter fractions were collected and assayed for lysosomal enzyme activity as described above. The percentage of total hydrolase activity eluted with Man-6-P–containing buffer (receptor bound fraction) was calculated. When noted, samples were pretreated with endoglycosidase H (New England Biolabs, Ipswich, MA), *Escherichia coli* alkaline phosphatase (Sigma-Aldrich), and/or recombinant uncovering enzyme as follows: plasma samples were incubated with 3000 U of endoglycosidase H for 2 h 30 min at 37°C under nonreducing conditions, with 15 U of alkaline phosphatase in alkaline phosphatase buffer (5 mM Tris-HCl, pH 8.0, 0.5 mM $MgCl_2$, and 0.5 mM $ZnCl_2$) for 18 h at 37°C and with 18 μg of uncovering enzyme for 2 h at 37°C, respectively.

Purification of Lysosomal Hydrolases from Mouse Plasma and Endocytosis Assay

Wild-type and UCE −/− acid hydrolases were purified from 4 mL plasma over a CI-MPR affinity column as described above. The Man-6-P–eluted fraction was extensively dialyzed against PBS and labeled with 0.5 mCi of ^{125}I (MP Biomedicals) in iodination tubes (Pierce Chemical, Rockford, IL) following the manufacturer's instructions. The free iodine was removed using a PD-10 desalting column (GE Healthcare), and iodinated hydrolases were purified again over the CI-MPR affinity column. After dialysis against PBS, the mix of acid hydrolases (200,000 cpm diluted in PBS/1% BSA) was incubated for 2 h at 37°C with mouse L cells either lacking the CI-MPR (clone D9) or stably transfected with full-length bovine CI-MPR (clone Cc2) (Lobel *et al.*, 1989). Cells were then rinsed and incubated for 30 s with 0.5 M NaCl and 0.2 M acetic acid, pH 3.5, to release the hydrolases bound to the cell surface. Finally, cells were lysed in 0.1 M NaOH, and the radioactivity that has been internalized was counted with a counter (Beckman Coulter LS 6000IC). Where indicated, ^{125}I-hydrolases purified from the UCE −/− plasma were pretreated for 2 h at 37°C with 72 μg of uncovering enzyme before incubation with the cells.

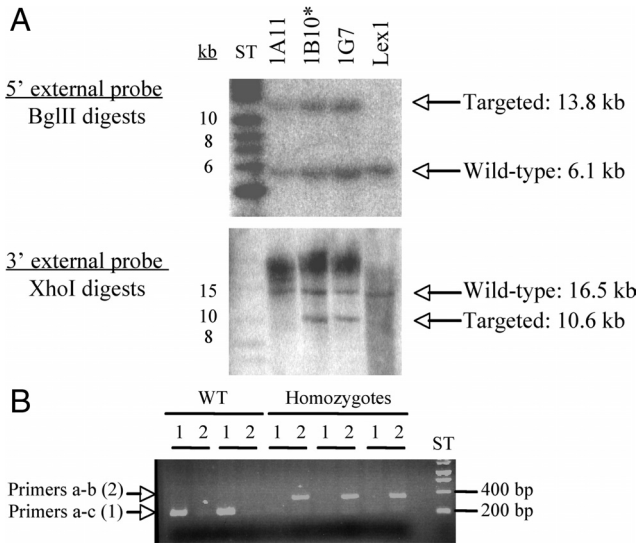

Figure 2. Generation of UCE deficient mice. (A) The targeting vector (engineered as described in *Materials and Methods*; Figure 1) was transformed into Lex1 ES cells and the successful insertion of the cassette into the targeted gene was assessed by Southern blotting. The genomic DNA was digested by either BglII or XhoI, and the resulting fragment was detected with a 5′ external probe or a 3′ external probe (see Figure 1), respectively. The 5′ probe detected a 6.1-kb band for the wild-type allele and a 13.8-kb band for the targeted allele. The 3′ probe detected a 16.5-kb fragment for the wild-type allele and a 10.6-kb fragment for the mutant allele. Clones 1B10 and 1G7, containing the mutant allele, were selected for the injection into C57BL\6 blastocysts. The mice derived from clone 1B10* achieved germline transmission. (B) The genotype of the mice was determined by PCR using primers complementary to sequences localized in exon 4 (a) and exon 5 (c) that flank the insertion site, and a primer complementary to the gentrap cassette (b) (see Figure 1). The first set of primers (a-c, lane 1) allows the amplification of an ~260-base pair fragment in the wild-type allele, whereas the second set (a-b, lane 2) amplifies an ~400-base pair fragment in the mutated allele.

RESULTS

Generation and Phenotypic Screening of the UCE-deficient Mice

A mouse deficient for the gene that encodes uncovering enzyme was generated by insertional mutagenesis. The targeting vector (Figure 1) was engineered as described in *Materials and Methods* and electroporated into ES cells. Correctly targeted clones were identified and confirmed by Southern blot analysis (Figure 2A) using a 289-base pair 5′ external probe (8/9) and a 236-base pair 3′ external probe (10/11) (Figure 1) to recognize the fragments generated after digestion of the genomic DNA by BglII or XhoI restriction enzymes, respectively (Figure 1). The 5′ external probe (8/9) detected a wild-type band of 6.1 kb or a mutant band of 13.8 kb, whereas the 3′probe (10/11) detected a wild-type band of 16.5 kb or a mutant band of 10.6 kb. Two targeted ES cell clones (1B10 and 1G7) were identified and microinjected into C57BL/6 (albino) blastocysts to generate chimeric animals that were bred to C57BL/6 (albino) females, and the result-

Table 1. Plasma levels of acid hydrolases in wild-type and UCE −/− mice (n ≥ 5)

	Activity (nmol/ml/h)		-Fold increase	
	Wild-type	UCE(−/−)	UCE(−/−)	GNPTAB(−/−)[a]
β-Hexosaminidase	272 ± 71	624 ± 121	2.3×	6.7×
α-Mannosidase	978 ± 153	3045 ± 384	3.1×	
β-Glucuronidase	11 ± 5	59 ± 18	5.4×	11.2×
β-Mannosidase	171 ± 31	293 ± 50	1.7×	9.4×
α-Galactosidase	24 ± 6	45 ± 9	1.9×	
β-Galactosidase	23 ± 9	37 ± 8	1.6×	13.9×
β-Glucocerebrosidase	49 ± 10	53 ± 11	1.1×	

[a] Data were collected from Gelfman *et al*. (2007).

ing heterozygous offspring were interbred to produce homozygous Nagpa-deficient mice. The genotyping of the mice was performed by PCR amplification of genomic DNA (Figure 2B) using primers that flank the insertion site (primers a and c) and a primer complementary to the genetrap cassette (b) (Figure 1). The first set of primers allowed the PCR amplification of an ~260-base pair fragment in wild-type but not in UCE −/−, whereas the second set of primers only amplified a band of ~400 base pairs from the UCE −/− cDNA containing the genetrap cassette (Figure 2).

On macroscopic examination, UCE-deficient mice were indistinguishable from wild-type littermates. The UCE-deficient mice were produced in a 1:2:1 Mendelian ratio; were anatomically normal; and showed normal growth rates, survival, and fertility. Standard serum chemistry and hematology workups were unremarkable (Supplemental Table S1). Behavioral tests (such as circadian rhythm, open field, inverted screen, prepulse inhibition of the acoustic startle response, tail suspension, marble burying, and context trace conditioning) gave similar results for both wild-type and UCE −/− mice. A comprehensive histologic survey of many tissues (including brain, liver, kidney, heart, lung, pancreas, spleen, stomach, intestines, salivary glands, chondrocytes, osteoclasts, osteoblasts, retina, and fibroblasts) did not reveal any detectable abnormalities.

Plasma Levels of Acid Hydrolases Are Elevated in UCE −/− Mice

Mice-deficient in GlcNAc-1-phosphotransferase activity exhibit 7- to 14-fold elevations in their plasma levels of acid hydrolases, as would be expected when the ability to synthe size the Man-6-P recognition marker is lost (Gelfman *et al*., 2007, Lee *et al*., 2007) (Table 1). To assess whether the loss of UCE gives rise to a similar phenotype, the activity of seven acid hydrolases was measured in the plasma of UCE −/− mice (Table 1). These assays revealed a 1.6- to 5.4-fold increase in the plasma level of these enzymes compared with wild-type mice except for β-glucocerebrosidase, which is known to traffic to lysosomes in a Man-6-P–independent manner (Reczek *et al*., 2007).

The steady-state levels of acid hydrolases in the blood are determined by the rate of secretion from cells along with the rate of clearance, especially by carbohydrate binding receptors such as the mannose receptor on macrophages and hepatic endothelial cells (Lee *et al*., 2002a). In this regard, the *N*-linked glycans of the acid hydrolases secreted by cells deficient in UCE activity would be expected to be mainly of the high-mannose type (putative mannose receptor ligands), whereas the *N*-linked glycans on the acid hydrolases synthesized by GlcNAc-1-phosphotransferase null cells are known to be of the complex-type[1] that are not recognized by this receptor (Maynard and Baenziger, 1981). Consequently, the lower level of acid hydrolases in the blood of UCE −/− mice compared with the GlcNAc-1-phosphotransferase −/− mice could be the result, at least in part, of a greater rate of clearance by the mannose receptor.

To investigate this possibility, the mannose receptor was blocked by injection of HSA-mannose into the tail vein of the various mouse types and the effect on the plasma level of several acid hydrolases was determined 4 h later. As shown in Figure 3A, this treatment resulted in a doubling of the level of β-galactosidase and β-hexosaminidase in wild-type mice with no effect on the level of β-mannosidase. By contrast, the blockade of the mannose receptor caused a sixfold increase in the level of β-galactosidase, a fourfold increase in β-hexosaminidase, and a twofold increase in β-mannosidase activity in the plasma of UCE −/− mice. As predicted, the HSA-mannose injection had little or no effect on the plasma levels of the hydrolases in GlcNAc-1-phosphotransferase (GNPTAB) −/− mice. These results indicate that the acid hydrolases secreted by cells of the UCE −/− mice are cleared from the plasma by mannose receptors more rapidly than the hydrolases secreted by the cells of wild-type mice or GlcNAc-1-phosphotransferase −/− mice. Therefore, the measurements of the steady-state levels of the acid hydrolases underestimate the rate of secretion by UCE −/− cells relative to that of the other types of mice. When this factor is taken into account, the hypersecretion of some acid hydrolases by UCE −/− cells approaches that observed with GlcNAc-1-phosphotransferase negative cells, especially for β-hexosaminidase (Figure 3B).

UCE −/− Fibroblasts Hypersecrete Cathepsin D

To directly determine the degree of acid hydrolases secretion by UCE −/− cells, skin fibroblasts were isolated and cathepsin D sorting was followed by pulse/chase analysis. Wild-type and UCE −/− cells were incubated with [^{35}S]methionine/cysteine for 1.5 h followed by a chase of 4 h in unlabeled medium containing 5 mM of Man-6-P to inhibit reinternalization of the secreted cathepsin D by the CI-MPR (Figure 4A) or 5 mM of Man-6-P and 10 μM HSA-mannose

[1] The difference in oligosaccharide structure arises because the presence of Man-6-P residues on high-mannose glycans prevents processing to complex type structures. Therefore, hydrolases that lack Man-6-P (as occurs in GlcNAc-1-phosphotransferase null cells) are processed to complex-type units.

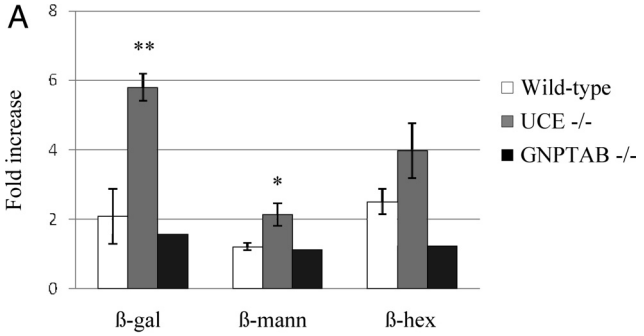

B

	ß-gal	ß-mann	ß-hex
Wild-type	2.1	1.2	2.5
UCE -/-	9.2	4.9	5.6
GNPTAB -/-	18.1	10.3	8.0

Figure 3. UCE −/− plasma acid hydrolases are rapidly cleared by the mannose receptor. (A) HSA-mannose (200 mg/kg) was injected in the tail vein of ~3-mo-old wild-type, UCE −/− or GNPTAB −/− mice. The activities of β-galactosidase (β-gal), β-mannosidase (β-mann), and β-hexosaminidase (β-hex) were measured in plasma samples collected before treatment (starting levels) and 4 h after injection. Relative increases (-fold) compared with starting levels (set to 1) are shown on the graph. Wild-type and UCE −/− mice, n = 4; GNPTAB −/− mice, n = 2. **$p < 0.001$, *$p < 0.01$. (B) Effect of the mannose receptor blockade on plasma acid hydrolases levels was calculated. Values represent the increases (-fold) in plasma β-gal, β-mann, or β-hex activities observed 4 h after injection of 200 mg/kg HSA-Man over wild-type basal levels (noninjected).

to block both the CI-MPR and the mannose receptor (Figure 4B). The cathepsin D was immunoprecipitated from cell lysates and chase media, subjected to SDS-PAGE, and visualized by autoradiography. As shown in Figure 4A, the wild-type fibroblasts sorted almost all the newly synthesized cathepsin D to lysosomes, as indicated by the 43-kDa species detected in the cell lysate, which results from the intralysosomal processing of the cathepsin D precursor into the intermediate form. The fibroblasts of the UCE −/− mice also sorted the majority of the cathepsin D to lysosomes but, in contrast to the wild-type cells, secreted readily detectable amounts of the 47-kDa proform into the medium. When the bands representing cathepsin D were excised, solubilized, and counted, the secretion of cathepsin D by the UCE −/− cells was found to be twice that of wild-type cells (21 ± 4 vs. 10 ± 3%; $p < 0.001$), but much less than the 63% secretion observed GlcNAc-1-phosphotransferase −/− fibroblasts (Lee *et al*., 2007). Similar results were obtained when HSA-mannose was added to the chase media (14 ± 3% of cathepsin D secreted from WT cells and 24 ± 3% from UCE −/− cells) (Figure 4B), suggesting that reinternalization of the secreted UCE −/− acid hydrolases by the mannose receptor was negligible.

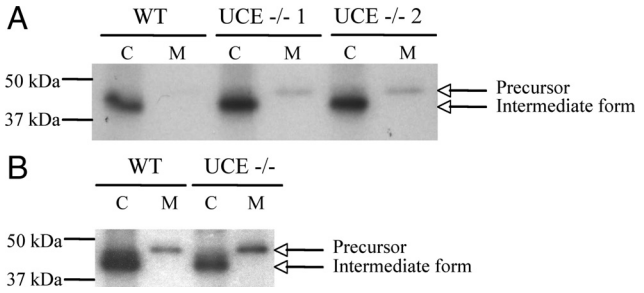

Figure 4. UCE −/− mouse skin fibroblasts hypersecrete cathepsin D. (A) Primary skin fibroblasts isolated from wild-type or UCE −/− mice were incubated for 90 min with TRAN ^{35}S-LABEL methionine/cysteine containing media (pulse) and then for 4 h in unlabeled media (chase) containing 5 mM of Man-6-P. Cathepsin D was immunoprecipitated from cell lysates (C) and media (M) collected at the end of the 4-h chase period and resolved on 10% SDS-PAGE. Signals were visualized by autoradiography. A representative experiment (of a total of 3 for WT and 6 for UCE −/−, with fibroblasts isolated from separate mice) is shown. Arrows indicate the proform of cathepsin D (~47 kDa) and cathepsin D intermediate form (43 kDa). (B) Fibroblasts were incubated for 90 min with TRAN ^{35}S-LABEL methionine/cysteine containing media and then for 4 h in unlabeled chase media containing 5 mM Man-6-P and 660 μg/ml HSA-mannose. Cathepsin D was immunoprecipitated as described in A (WT and UCE −/−, n = 3).

Acid Hydrolases Are Efficiently Targeted to Lysosomes in Brain and Liver of UCE −/− Mice

The ability of the acid hydrolases to reach lysosomes in the absence of UCE activity was further investigated using brain and liver from mice that had been perfused with PBS to remove blood from their organs. Table 2 shows that the acid hydrolase content of these organs from UCE −/− mice was indistinguishable from that of the wild-type mice. To determine whether the hydrolases were actually in lysosomes, membrane fractions of brain and liver were fractionated on 18% self-forming Percoll density gradients, which separate dense lysosomes (bottom of the gradient) from the other subcellular organelles that concentrate in the lightest fractions of the gradient. The activity of four acid hydrolases was measured in the seven fractions collected after centrifugation and expressed as a percentage of the total activity recovered. Figure 5B shows that the distribution of β-galactosidase on the gradient was almost identical in the brain from both wild-type and UCE −/− mice, with a strong concentration in the dense lysosome fraction. Similar results were observed for β-mannosidase, β-hexosaminidase, and β-glucuronidase. The acid hydrolase levels in this last fraction were slightly decreased in the UCE −/− liver compared with wild-type (i.e., β-galactosidase; Figure 5A). Together, these findings indicate that acid hydrolase targeting to lysosomes in the brain of UCE −/− mice is equivalent to that of wild-type mice and only slightly, if at all, impaired in the liver.

Acid Hydrolases in UCE −/− Mouse Plasma Bind to CI-MPR In Vitro

In the absence of UCE activity, lysosomal hydrolases would be expected to bear *N*-linked high mannose glycans with GlcNAc-P-Man diesters unless the GlcNAc residues are removed by an alternative pathway. To determine the state of the phosphorylated glycans on the acid hydrolases produced by UCE −/− cells, we analyzed the binding of plasma acid hydrolases to a CI-MPR affinity column under various conditions. In brief, plasma samples (50–100 μl) were diluted with buffer, loaded onto the column, and the amount of acid hydrolase (% of starting material) that passed through the column, bound nonspecifically, and eluted with Glc-6-P or bound specifically and required Man-6-P for elution, was determined. The results for three acid hydrolases are shown in Table 3A. (NB. The total levels of the hydrolases in the plasma of the WT and UCE −/− mice are given in Table 1.) It is apparent that a fraction of all three hydrolases from both wild-type and UCE −/− mouse plasmas bound specifically to the CI-MPR affinity column, but

Table 2. Levels of acid hydrolases in the brain and liver of wild-type and UCE −/− mice

	Activity (nmol/ml/h)			
	Wild-type brain (n = 4)	UCE −/− brain (n = 6)	Wild-type liver (n = 4)	UCE −/− liver (n = 4)
β-Hexosaminidase	28.0 ± 7.3	28.1 ± 6.5	15.7 ± 5.7	22.1 ± 4.9
β-Glucuronidase	6.0 ± 1.3	5.9 ± 1.1	34.1 ± 12.7	40.5 ± 26.1
β-Mannosidase	4.6 ± 1.6	5.7 ± 4.9	14.9 ± 8.1	10.5 ± 7.2
β-Galactosidase	9.4 ± 3.3	12.1 ± 3.4	20.1 ± 7.9	26.9 ± 10.0

the extent of binding of the β-mannosidase and β-glucuronidase varied substantially between wild-type and UCE −/−. Thus, β-mannosidase from UCE −/− plasma bound 9% compared with 50% for the wild-type enzyme and β-glucuronidase from the UCE −/− and wild-type plasma samples bound 79 and 49%, respectively. Similar amounts of β-hexosaminidase binding (12%) were observed with both types of plasma. The binding of all three WT and UCE −/− hydrolases to the affinity column was mediated by residues exposed on high-mannose sugar chains, because binding was abolished when samples were pretreated with endoglycosydase H (Table 3A, Endo H). It should be noted that the hydrolases in the plasma may originate by direct secretion from cells or by release from lysosomes in which they would have been exposed to glycosidase and phosphatase activities that have the ability to excise the GlcNAc and phosphate residues from GlcNAc-P-Man and Man-6-P, respectively (Varki and Kornfeld, 1980, Sun *et al*., 2008). The ratio of the acid hydrolases that are directly secreted via the Golgi (with intact oligosaccharide chains) compared with the acid hydrolases that are released after traffic through the lysosome may differ between the wild-type and UCE −/− hydrolases. Consequently, the binding percentages of the wild-type and UCE −/− acid hydrolases to the CI-MPR affinity column cannot be used to compare their relative affinity for the receptor in vivo.

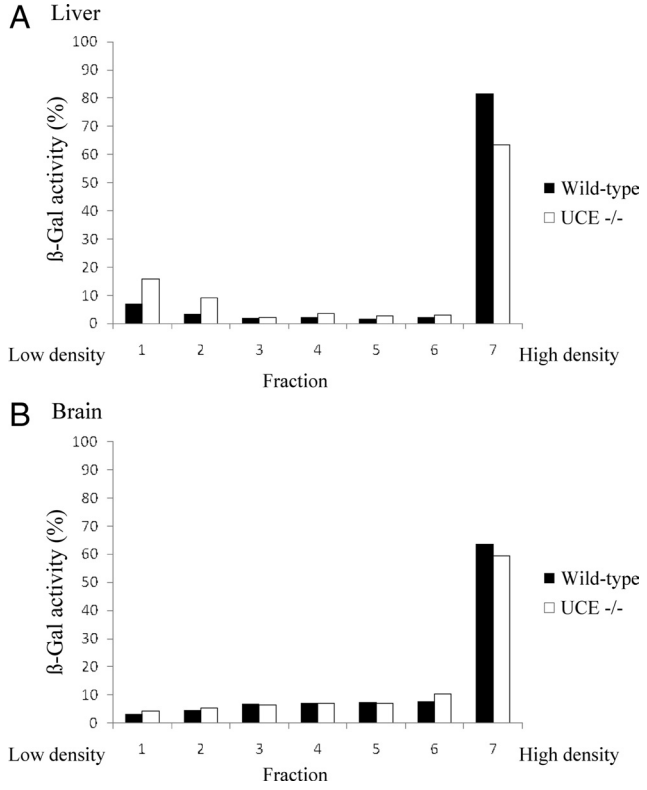

Figure 5. The subcellular distribution of acid hydrolases in the brain and liver of wild-type and UCE −/− mouse is similar in a self-forming Percoll density gradient. Wild-type or UCE −/− liver (A) and brain (B) were homogenized in isotonic sucrose with a Potter-Elvehjem homogenizer and centrifuged at 1000 × *g* to prepare a postnuclear supernatant (PNS). The PNS was subjected to centrifugation at 35,000 rpm in a 50Ti rotor for 40 min at 4°C to obtain a membrane fraction, which was resuspended in isotonic sucrose and loaded on top of a 18% Percoll solution. Self-forming gradients were generated by centrifugation at 25,000 rpm in a SW55Ti rotor for 40 min at 4°C. Seven fractions were collected from the top (low density) to the bottom (densest fraction), and acid hydrolase content was determined by enzyme assays. Graphs represent the distribution of β-galactosidase in WT (n = 2) or UCE −/− (n = 2) liver (A) and brain (B), expressed as a percentage of the total activity recovered in each fraction. Similar distributions were observed for β-hexosaminidase, β-glucuronidase, and β-mannosidase.

Treatment of the wild-type plasma with alkaline phosphatase (Table 3A, Alk.phos.) decreased binding of the three hydrolases by 67–90%, indicating that the binding was mostly mediated by Man-6-P monoesters. By contrast, the alkaline phosphatase treatment had no effect on the binding of β-mannosidase and β-glucuronidase present in the UCE −/− mouse plasma, consistent with these hydrolases containing glycans with Man-6-P diesters. This conclusion was supported by the finding that the binding of these two hydrolases to the CI-MPR affinity column was enhanced after treatment with purified UCE (71% binding for β-mannosidase and 88% binding for β-glucuronidase). When UCE treatment was followed by incubation with alkaline phosphatase, binding of these two hydrolases to the column was greatly decreased, as expected if the UCE was converting diesters to monoesters that are susceptible to alkaline phosphatase action. The β-hexosaminidase in the UCE −/− mouse plasma behaved as if it contained both Man-6-P monoesters and diesters. Thus, alkaline phosphatase treatment decreased binding from 12 to 3%, whereas UCE treatment increased the binding to 36%. One possibility is that the β-hexosaminidase consists of molecules directly secreted by cells and molecules that are derived from lysosomes (uncovered by lysosomal α-*N*-acetylglucosaminidase). Treatment of the acid hydrolases in wild-type mouse plasma with UCE did not enhance binding to the CI-MPR affinity column, demonstrating that these enzymes lack GlcNAc-P-Man diesters.

In a second approach, the plasma samples were loaded onto the affinity column in the presence of either 200 μM Man-6-P or 10 mM GlcNAc-P-α-methylmannose (Table 3B). Binding of the acid hydrolases from wild-type mouse plasma was strongly inhibited by the Man-6-P (50–10% for β-mannosidase, 49–12% for β-glucuronidase, and 12–0% for β-hexosaminidase), whereas the GlcNAc-P-α-methylmannose had no effect, consistent with these hydrolases bearing Man-6-P monoesters exclusively. By contrast, the binding of

Table 3. Percentage of plasma acid hydrolases that specifically bind to a CI-MPR affinity column (1 representative experiment, n = 3)

A. Effect of endoglycosydase H, alkaline phosphatase (Alk.phos.), and uncovering enzyme treatment

	Wild-type					UCE −/−				
	Untreated	Endo H[a]	Alk.phos.	UCE	UCE + Alk.phos.	Untreated	Endo H[a]	Alk.phos.	UCE	UCE + Alk.phos.
β-Mannosidase	50	0	12	41	2	9	0	9	71	14
β-Glucuronidase	49	0	5	47	8	79	0	77	88	34
β-Hexosaminidase	12	3	4	8	1	12	1	3	36	3

B. Inhibition of binding by Man-6-P (M6P) or GlcNAc-P-α-methylmannose

	Wild-type				UCE −/−				
	Untreated	200 μM M6P	10 mM GlcNAc-P-α-methylman	1 mM M6P	Untreated	200 μM M6P	10 mM GlcNAc-P-α-methylman	1 mM M6P	200 μM M6P + 10 mM GlcNAc-P-α-methylman
β-Mannosidase	50	10	49	0	9	14	1	1	1
β-Glucuronidase	49	17	50	11	79	82	50	65	28
β-Hexosaminidase	12	0	14	3	12	6	5	4	3

[a] n = 2.

the β-mannosidase and β-glucuronidase from UCE −/− mouse plasma was not affected by 200 μM Man-6-P but was inhibited by the GlcNAc-P-α-methylmannose (9–1% for the β-mannosidase and 79–50% for the β-glucuronidase), indicative of the presence of Man-6-P diesters on these hydrolases. Binding of the β-hexosaminidase from the UCE −/− mouse plasma to the affinity column was partially inhibited by both Man-6-P and GlcNAc-P-α-methylmannose, consistent with it containing both Man-6-P monoesters and diesters. Note that 1 mM Man-6-P inhibited binding of both wild-type and UCE −/− hydrolases, although UCE −/− β-glucuronidase binding remained higher (65%) than when inhibited by GlcNAc-P-α-methylmannose (50%). A combination of both Man-6-P (200 μM) and GlcNAc-P-α-methylmannose (10 mM) decreased the binding of this enzyme to 28%.

Taken together, these data strongly indicate that the acid hydrolases of wild-type mice contain Man-6-P monoesters, whereas the hydrolases of the UCE −/− mice contain GlcNAc-P-Man diesters and have a decreased affinity for the CI-MPR compared with monoesters-containing enzymes (i.e., the enhanced binding measured after UCE treatment).

Acid Hydrolases in UCE −/− Mouse Plasma Fail to Bind to CD-MPR In Vitro

In a study of the ligand-binding properties of the CI-MPR and the CD-MPR, it was found that the CI-MPR binds GlcNAc-P-α-methylmannose with low affinity (K_d of 1×10^{-4} vs. 7×10^{-6} for Man-6-P), whereas binding of this diester to the CD-MPR was below detectable level ($K_d > 4 \times 10^{-3}$) (Tong and Kornfeld, 1989). More recently, surface plasmon resonance studies demonstrated that the CD-MPR has little affinity for acid α-glucosidase when it only exposes GlcNAc-P-Man diesters (Chavez *et al.*, 2007). To determine whether UCE −/− mouse plasma acid hydrolases that bear phosphodiesters are able to bind to the CD-MPR, plasma samples from wild-type and UCE −/− mice were passed over a CD-MPR affinity column and the binding of three acid hydrolases was measured. Although 6% of the β-mannosidase, 13% of the β-glucuronidase, and 6% of the β-hexosaminidase from wild-type plasma bound specifically to the affinity column, <2% of these hydrolases from UCE −/− mouse plasma bound (Table 4). This is consistent with the CD-MPR not being able to bind Man-6-P diesters.

Acid Hydrolases of UCE −/− Mouse Plasma Are Poorly Internalized by Mouse L Cells Expressing the CI-MPR

Because the CI-MPR affinity chromatography experiments use columns with high levels of bound CI-MPR, we wanted to determine the ability of acid hydrolases containing Man-6-P diesters to bind to the receptor under more physiological conditions. To do this, acid hydrolases were purified from the plasma of wild-type and UCE −/− mice on the CI-MPR affinity column, labeled with ^{125}I and incubated with mouse L cells that either lack or express the CI-MPR. The radioactivity internalized after incubation of the WT or UCE −/− plasma ^{125}I-hydrolases with the cells (CTRL cells or CI-MPR–expressing cells) for a 2-h period at 37°C was determined and the nonspecific uptake by the receptor-deficient cells was set to 1 (Figure 6). We selected plasma as the source for the hydrolases based on the finding that the plasma hydrolases of the UCE −/− mice still contained GlcNAc-P-Man diesters (Table 3). The acid hydrolases in the tissues of these mice are mainly localized to lysosomes where they are exposed to α-*N*-acetylglucosaminidase that cleaves the GlcNAc and thereby converts the diesters to monoesters. In tissues others than the brain, the Man-6-P residues are then hydrolyzed by a phosphatase to give rise

Table 4. Binding of wild-type or UCE −/− plasma acid hydrolases to a CD-MPR affinity column (1 representative experiment, n = 3)

	Wild-type	UCE −/−
β-Mannosidase	6	<2
β-Glucuronidase	13	<2
β-Hexosaminidase	6	<2

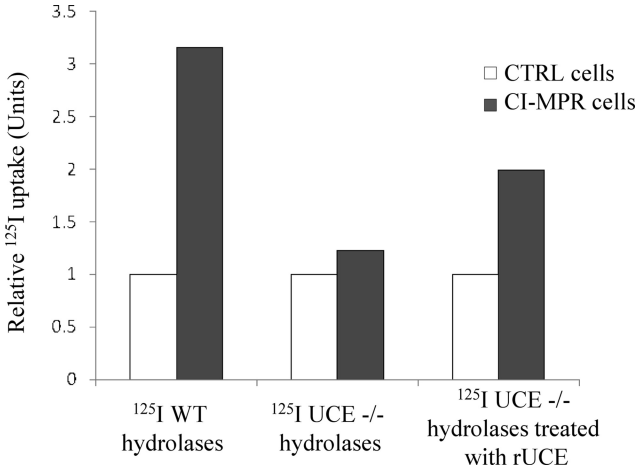

Figure 6. UCE −/− plasma acid hydrolases are poorly internalized by CI-MPR–expressing mouse L cells. Plasma acid hydrolases (wild-type or UCE −/−) were enriched over a CI-MPR affinity column and then labeled with ^{125}I and incubated with D9 cells lacking CI-MPR (CTRL cells, n = 3) or Cc2 cells stably transfected with bovine CI-MPR (CI-MPR cells, n = 3). The mix of acid hydrolases (200,000 cpm) was added in a 36-mm well and incubation was performed for 2 h at 37°C. The amount of radioactivity internalized by CTRL cells (<0.5% of total) was set to 1 (nonspecific uptake), and the amount of ^{125}I-hydrolases specifically internalized by CI-MPR cells was expressed as relative uptake over CTRL cells. One representative experiment is shown. Where indicated, UCE −/− ^{125}I-labeled hydrolases were treated for 2 h at 37°C with uncovering enzyme before incubation with the cells (one representative experiment with n = 2).

to neutral species (Sun *et al*., 2008). Therefore, plasma is the best source for "native" enzymes. Although the relative levels of the various acid hydrolases differed between the plasmas of the WT and UCE −/− animals (Table 1) along with their efficiency of binding to the CI-MPR affinity column, the purified hydrolases represented the molecules with the highest affinity for the CI-MPR and therefore had the highest likelihood of being internalized by the CI-MPR–expressing cells. Our results show that the CI-MPR–expressing L cells internalized the acid hydrolases of wild-type plasma at 3 times the rate of the receptor-deficient cells. The acid hydrolases of the UCE −/− plasma were internalized about equally by both types of L cells. Pretreatment of the UCE −/− sample with purified UCE resulted in increased internalization by the CI-MPR–expressing L cells. As with our in vitro binding studies, this result shows that conversion of phosphomannose diesters to monoesters significantly increases the affinity of UCE −/− hydrolases for the CI-MPR. It should be noted that in this experiment the amount of wild-type hydrolases internalized by the CI-MPR–expressing cells was quite low (<0.5% of total). Consequently, this assay may not be sufficiently sensitive to detect GlcNAc-P-Man–dependent internalization of the UCE −/− hydrolases, as uptake of theses enzymes would be expected to be less efficient compared with hydrolases with Man-6-P monoesters. Because cathepsin D was sorted to lysosomes with good efficiency in the UCE −/− fibroblasts (Figure 4), hydrolases containing Man-6-P diesters must be able to bind to the CI-MPR under the conditions of the TGN environment.

DISCUSSION

The data presented here demonstrate that inactivation of the gene that encodes UCE in mice results in an inability to convert GlcNAc-P-Man diesters to monoesters on newly synthesized acid hydrolases. This finding indicates that UCE accounts for virtually all of the uncovering activity in the Golgi. The small amount of Man-6-P monoesters found on the β-hexosaminidase present in the plasma of the UCE −/− animals probably is the result of cleavage of the GlcNAc in the lysosome by α-*N*-acetylglucosaminidase (Varki and Kornfeld, 1980), followed by the release of the lysosomal content into the circulation. Whether the phosphodiesters on β-mannosidase and β-glucuronidase are less sensitive to the action of the lysosomal α-*N*-acetylglucosaminidase or whether a smaller proportion of these enzymes originates from the lysosomal compartment is unknown.

The failure of the UCE −/− cells to convert the Man-6-P diesters to monoesters resulted in the hypersecretion of the acid hydrolases into the plasma, although the steady-state levels of these enzymes in the plasma did not reach the levels observed in mice that lack GlcNAc-1-phosphotransferase and therefore are completely unable to synthesize Man-6-P on their acid hydrolases. There are several reasons for this difference. First, the hydrolases in the plasma of the UCE −/− mice are rapidly cleared by the mannose receptor, whereas the hydrolases of the GlcNAc-1-phosphotransferase null mice fail to bind to this receptor. When this difference in clearance rate is taken into account, the degree of hypersecretion of some acid hydrolases by UCE −/− cells approaches that of the GlcNAc-1-phosphotransferase null cells. Second, the acid hydrolases synthesized by the UCE −/− cells bind to the CI-MPR, albeit with a lower affinity compared with Man-6-P monoesters, whereas the hydrolases of the GlcNAc-1-phosphotransferase null mice fail to interact with this receptor. We postulate that the weak binding of the acid hydrolases of the UCE −/− mice to the CI-MPR diverts some of the newly synthesized acid hydrolases from the secretory pathway to the endosome/lysosome targeting pathway. This is illustrated by the UCE −/− skin fibroblasts that target cathepsin D to lysosomes much more efficiently than occurs in GlcNAc-1-phosphotransferase null fibroblasts. However, it should be pointed out that the acid hydrolases of the UCE −/− mice do not bind to the CD-MPR. It has been reported that although most cell types express both the CI-MPR and the CD-MPR, some cell types such as Kupffer cells, selectively express the CD-MPR (Waguri *et al*., 2001). Such cell types are candidates for hypersecretion of acid hydrolases in the UCE −/− mice plasma.

The basis for the weak binding of the acid hydrolases carrying GlcNAc-P-Man diesters to the CI-MPR has been identified by recent studies of this receptor. The CI-MPR contains 15 repeating domains in its extracytoplasmic region and it has been established that domains 3 and 9 bind Man-6-P monoesters with high affinity (for review, see Dahms *et al*., 2008). A low-affinity binding site for Man-6-P was also identified within domain 5 (Reddy *et al*., 2004). Recently, it was reported that domain 5 has a preference for GlcNAc-P-Man diesters over Man-6-P monoesters, although the binding of this ligand is also of low affinity compared with the binding of Man-6-P to domain 9 (Chavez *et al*., 2007). This was shown using α-acid glucosidase containing *N*-linked oligosaccharides with either GlcNAc-P-Man diesters or Man-6-P monoesters. In this assay, the binding of α-acid glucosidase containing Man-6-P diesters to domain 5 was inhibited by GlcNAc-P-α-methylmannose (K_i = 1 mM), whereas the K_i for Man-6-P was 14 mM. These findings indicate that the interaction of the acid hydrolases of the UCE −/− mice with the CI-MPR is likely mediated via binding to domain 5 of the receptor. Nevertheless, a minor contribution of another binding domain to the overall bind-

ing avidity of the hydrolases to the CI-MPR cannot be ruled out. The hydrolases that were analyzed in our study have two or more *N*-linked glycans, each of which can contain one or two GlcNAc-P-Man residues. For example, mouse β-glucuronidase is a tetramer with three *N*-linked glycans per monomer, most of which are phosphorylated (Shipley *et al*., 1993), which could explain why this hydrolase binds so efficiently to the CI-MPR affinity column. Interestingly, the binding of the β-glucuronidase in the UCE −/− plasma to the CI-MPR was more inhibited by a mixture of Man-6-P and GlcNAc-P-α-methylmannose than by GlcNAc-P-α-methylmannose alone. This observation supports the possibility that a weak binding of some *N*-glycans to domains 3 and/or 9 of the CI-MPR may strengthen/stabilize the interaction of the UCE −/− enzymes with the CI-MPR, although the involvement of domain 9 seems highly unlikely because it does not bind the diester-enriched form of α-acid glucosidase (Chavez *et al*., 2007).

Although the UCE −/− mice exhibit significant missorting of their newly synthesized acid hydrolases, this defect was not accompanied by the development of any of the tissue abnormalities seen in the GlcNAc-1-phosphotransferase null mice (Gelfman *et al*., 2007; Vogel *et al*., 2009). These mice are small, develop severe retinal degeneration and have striking inclusions in the secretory cells of the exocrine glands that are readily detectable at the light microscope level (Gelfman *et al*., 2007; Vogel *et al*., 2009). The most likely explanation for this difference is that the weak binding of the newly synthesized acid hydrolases to the CI-MPR in UCE −/− cells leads to the targeting of sufficient amounts of acid hydrolases to lysosomes in critical cell types to prevent pathological changes. These findings indicate that it is unlikely that UCE deficiency in humans would result in a phenotype as deleterious as occurs in patients with mucolipidosis type II and III.

ACKNOWLEDGMENTS

We thank Dr. William Canfield for generously providing HSA-mannose, purified UCE, and GlcNAc-1-phosphotransferase enzymes. We also thank Walter Gregory (Washington University, St. Louis, MO) for preparing the cathepsin D polyclonal antibody and the CI-MPR affinity column and Dr. Linda Olson (Medical College of Wisconsin, Milwaukee, WI) for the production of the CD-MPR affinity column. Finally, we thank Drs. Wang-Sik Lee, Jennifer Govero, Intaek Lee, and Balraj Doray for technical advice. This work was supported by National Institutes of Health grant CA-08759 (to S. K.).

REFERENCES

BeltrandelRio, H., Kern, F., Lanthorn, T., Oravecz, T., Piggott, J., Powell, D., Ramirez-Solis, R., Sands, A. T., and Zambrowicz, B. P. (2003). Saturation screening of the druggable mammalian genome. In: Model Organisms in Drug Discovery, ed. P. M. Carroll and K. Fitzgerald, Chichester, United Kingdom: John Wiley & Sons, 251–279.

Braulke, T., and Bonifacino, J. S. (2009). Sorting of lysosomal proteins. Biochim. Biophys. Acta *1793*, 605–614.

Cathey, S. S., Leroy, J. G., Wood, T., Eaves, K., Simensen, R. J., Kudo, M., Stevenson, R. E., and Friez, M. J. (2009). Phenotype and genotype in mucolipidosis II and III alpha/beta: a study of 61 probands. J. Med. Genet. (*in press*).

Chavez, C. A., Bohnsack, R. N., Kudo, M., Gotschall, R. R., Canfield, W. M., and Dahms, N. M. (2007). Domain 5 of the cation-independent mannose 6-phosphate receptor preferentially binds phosphodiesters (mannose 6-phosphate N-acetylglucosamine ester). Biochemistry *46*, 12604–12617.

Dahms, N. M., Olson, L. J., and Kim, J. J. (2008). Strategies for carbohydrate recognition by the mannose 6-phosphate receptors. Glycobiology *18*, 664–678.

Do, H., Lee, W. S., Ghosh, P., Hollowell, T., Canfield, W., and Kornfeld, S. (2002). Human mannose 6-phosphate-uncovering enzyme is synthesized as a proenzyme that is activated by the endoprotease furin. J. Biol. Chem. *277*, 29737–29744.

Gelfman, C., Vogel, P., Issa, T. M., Turner, A., Lee, W. S., Kornfeld, S., and Rice, D. S. (2007). Mice lacking α/β subunits of GlcNAc-1-phosphotransferase exhibit growth retardation, retinal degeneration, and secretory cell lesions. Invest. Ophthalmol. Vis. Sci. *48*, 5221–5228.

Ghosh, P., Dahms, N. M., and Kornfeld, S. (2003). Mannose 6-phosphate receptors: new twists in the tale. Nat. Rev. Mol. Cell Biol. *4*, 202–212.

Kornfeld, R., Bao, M., Brewer, K., Noll, C., and Canfield, W. (1999). Molecular cloning and functional expression of two splice forms of human *N*-acetylglucosamine-1-phosphodiester α-N-acetylglucosaminidase. J. Biol. Chem. *274*, 32778–32785.

Kornfeld, S., and Sly, W. S. (2000). I-cell disease and pseudo-Hurler polydystrophy: disorders of lysosomal enzyme phosphorylation and localization. In: The Metabolic and Molecular Bases of Inherited Disease, ed. C. R. Scriver, A. R. Beaudet, W. Sly, and D. Valle, New York: McGraw-Hill, 3469–3483.

Lee, S. J., Evers, S., Roeder, D., Parlow, A. F., Risteli, J., Risteli, L., Lee, Y. C., Feizi, T., Langen, H., and Nussenzweig, M. C. (2002a). Mannose receptor-mediated regulation of serum glycoprotein homeostasis. Science *295*, 1898–1901.

Lee, W. S., Payne, B. J., Gelfman, C. M., Vogel, P., and Kornfeld, S. (2007). Murine UDP-GlcNAc:lysosomal enzyme *N*-acetylglucosamine-1-phosphotransferase lacking the gamma-subunit retains substantial activity toward acid hydrolases. J. Biol. Chem. *282*, 27198–27203.

Lee, W. S., Rohrer, J., Kornfeld, R., and Kornfeld, S. (2002b). Multiple signals regulate trafficking of the mannose 6-phosphate-uncovering enzyme. J. Biol. Chem. *277*, 3544–3551.

Lobel, P., Fujimoto, K., Ye, R. D., Griffiths, G., and Kornfeld, S. (1989). Mutations in the cytoplasmic domain of the 275 kDa mannose 6-phosphate receptor differentially alter lysosomal enzyme sorting and endocytosis. Cell *57*, 787–796.

Maynard, Y., and Baenziger, J. (1981). Oligosaccharide specific endocytosis by isolated rat hepatic reticuloendothelial cells. J. Biol. Chem. *256*, 8063–8068.

Reczek, D., Schwake, M., Schröder, J., Hughes, H., Blanz, J., Jin, X., Brondyk, W., Van Patten, S., Edmunds, T., and Saftig, P. (2007). LIMP-2 is a receptor for lysosomal mannose 6-phosphate-independent targeting of beta-glucocerebrosidase. Cell *16*, 770–783.

Reddy, S. T., Chai, W., Childs, R. A., Page, J. D., Feizi, T., and Dahms, N. M. (2004). Identification of a low affinity mannose 6-phosphate-binding site in domain 5 of the cation-independent mannose 6-phosphate receptor. J. Biol. Chem. *279*, 38658–38667.

Reddy, S. T., Kumar, S. N., Haas, A. L., and Dahms, N. M. (2003). Biochemical and functional properties of the full-length cation-dependent mannose 6-phosphate receptor expressed in *Pichia pastoris*. Biochem. Biophys. Res. Commun. *309*, 643–651.

Rohrer, J., and Kornfeld, R. (2001). Lysosomal hydrolase mannose 6-phosphate uncovering enzyme resides in the *trans*-Golgi network. Mol. Biol. Cell *12*, 1623–1631.

Shipley, J. M., Grubb, J. H., and Sly, W. S. (1993). The role of glycosylation and phosphorylation in the expression of active human β-glucuronidase. J. Biol. Chem. *268*, 12193–12198.

Sun, P., Sleat, D. E., Lecocq, M., Hayman, A. R., Jadot, M., and Lobel, P. (2008). Acid phosphatase 5 is responsible for removing the mannose 6-phosphate recognition marker from lysosomal proteins. Proc. Natl. Acad. Sci. USA *105*, 16590–16595.

Tong, P. Y., and Kornfeld, S. (1989). Ligand interactions of the cation-independent mannose 6-phosphate receptor. Comparison with the cation-independent mannose 6-phosphate receptor. J. Biol. Chem. *264*, 7970–7975.

Varki, A., and Kornfeld, S. (1980). Identification of a rat liver α-*N*-acetylglucosaminyl phosphodiesterase capable of removing "blocking" α-*N*-acetylglucosamine residues from phosphorylated high mannose oligosaccharides of lysosomal enzymes. J. Biol. Chem. *255*, 8398–8401.

Varki, A., and Kornfeld, S. (1981). Purification and characterization of rat liver α-N-acetylglucosaminyl phosphodiesterase. J. Biol. Chem. *256*, 9937–9943.

Varki, A., and Kornfeld, S. (1983). The spectrum of anionic oligosaccharides released by endo-β-N-acetylglucosaminidase H from glycoproteins. J. Biol. Chem. *258*, 2808–2818.

Vogel, P., Payne, B. J., Read, R., Lee, W. S., Gelfman, C. M., and Kornfeld, S. (2009). Comparative pathology of murine mucolipidosis types II and IIIC. Vet. Pathol. *46*, 313–324.

Waguri, S., Kohmura, M., Kanamori, S., Watanabe, T., Ohsawa, Y., Koike, M., Tomiyama, Y., Wakasugi, M., Kominami, E., and Uchiyama, Y. (2001). Different distribution patterns of the two mannose 6-phosphate receptors in rat liver. H. Histochem. Cytochem. *49*, 1397–1405.

Zambrowicz, B. P., *et al*. (2003). Wnk1 kinase deficiency lowers blood pressure in mice: a gene-trap screen to identify potential targets for therapeutic intervention. Proc. Natl. Acad. Sci. USA *100*, 14109–14114.